

Final Draft
of the original manuscript:

Evadzi, P.I.K.; Zorita, E.; Huenicke, B.:
**West African sea level variability under a changing climate - What can we
learn from the observational period?**
In: Journal of Coastal Conservation. Vol. 23 (2019) 4, 759 - 771.
First published online by Springer: August 06, 2019

DOI: 10.1007/s11852-019-00704-z
<https://dx.doi.org/10.1007/s11852-019-00704-z>

**WEST AFRICAN SEA LEVEL VARIABILITY
UNDER A CHANGING CLIMATE –WHAT CAN WE LEARN
FROM THE OBSERVATIONAL PERIOD?**

Prosper I.K. Evadzi ^{*+}, Eduardo Zorita⁺ and Birgit Hünicke⁺

(+) Helmholtz-Zentrum Geesthacht, Institute of Coastal Research, Germany

(*) Brockmann Consult GmbH, Chrysanderstr. 1, D-21029 Hamburg, Germany

(Corresponding author) prosper.evadzi@brockmann-consult.de

ACKNOWLEDGMENT

This research received funding support from the Deutscher Akademischer Austauschdienst (DAAD) and the Institute of Coastal Research (Helmholtz-Zentrum Geesthacht). This research appreciates the support of the Ghana Survey Department, Permanent Service for Mean Sea Level (PSMSL) and other institutions for making data available for this research.

ABSTRACT

This study focuses on mean sea-level variability at the West African coast in the observational period (1993-2013) and its offshore waters, investigating its decadal variability, long-term trends and the large-scale climate patterns that are connected to its variability.

To achieve this objective, statistical analyses are performed on several available data sets: sea-level data from tide gauges (Takoradi, Tema and Forcados), satellite altimetry (combined TOPEX/Poseidon, Jason-1 and Jason-2/OSTM), gridded sea-level reconstruction (Church et al. 2004), meteorological reanalysis (NCEP), a high-resolution ocean model simulation driven by this meteorological reanalysis, and, observational data sets (The Hadley Centre Global Sea Ice and Sea Surface Temperature (HadISST1), and the Atlantic Multi-decadal Oscillation (AMO) index).

Ghana is the only country along the West African coast with two relatively long sea-level records available (Takoradi and Tema), but with data quality concerns (Woodworth et al. 2007). Attempts are made to combine these two records, which cover different but overlapping periods, to construct a regional sea-level curve for Ghana (1929-1981) that may be regionally representative.

A physical connection is identified between the AMO, sea-surface temperature and sea level in the Gulf of Guinea and mean sea-level trends and variability of the West African coast. It has been found that a stronger AMO is connected with higher mean sea level in the Tropical Atlantic and in particular also at the Gulf of Guinea sea level. This connection may explain the multidecadal variability of sea level there, and in particular the negative trends between 1955 and 1975 and the positive trends thereafter. In addition, warmer sea surface temperatures in the Gulf of Guinea are also connected with higher sea level, although a simple estimation based on reasonable assumptions of the thermal expansion of the water column is not sufficient to explain the connection between sea-surface-temperature and sea-level. More detailed modelling studies will be needed to explain this link.

Although this study provides useful information for adaptation strategies in Ghana, the research is unable to provide sea-level information between the years 1981 and 1993 because of lack of data.

KEYWORDS: Regional Sea-level Rise, Sea-level Variability, Climate Change, Climate Change Adaptation, Coastal Impacts

INTRODUCTION

Variations in the external climate forcing, like the increase in atmospheric greenhouse gases, affect the radiation balance of the planet and is reflected in global and regional sea-level changes (Stammer et al. 2013; Church et al. 2013; Anthoff et al. 2006). In addition to external forcing, internal climate variability usually organized in large-scale spatial patterns, such as the El Niño-Southern Oscillation (ENSO) and the Atlantic Multidecadal Variability (AMO), may also affect the decadal and multi-decadal variability of sea-level at regional scales. In the Northern Hemisphere, sea-level trends and variability have been a subject of multiple studies, as most of the long-tide-gauges are located there. In contrast, the Southern Hemisphere provides very few long, multidecadal, -records. Recently the weight of the Southern Hemisphere for the estimation of global sea-level rise and its acceleration over the 20th century has been recently recognized. Here, we focus on a sea-level variability and trends in a region that has been so far barely studied, the Gulf of Guinea, using the very few tide-gauge records from Ghana, satellite altimetry and a global high-resolution ocean-only simulation covering approximately the past 50 years driven by meteorological reanalysis. The focus of this paper lies on the Gulf of Guinea (GoG) and in particular on the coast of Ghana. Our aims are twofold: to investigate the connections between sea-level in this region and large-scale climate variability, and (2) to improve the historical sea-level data from tide-gauges in this region to provide a more accurate, although still uncertain, estimation of the sea-level trend in this region.

The estimated global mean sea-level (GMSL) rise since the mid-19th century has been estimated to be in the range of about 1.3 to 1.7 mm/year in the last report by the Intergovernmental Panel on Climate Change (IPCC 2013). This rise is likely to have increased since 1993 to a rate of about was 3.2 [2.8 to 3.6] mm/year (IPCC 2013), although it has to be borne in mind that both estimations rely on data of different nature, tide gauges versus satellite altimetry. The estimation of global sea-level rise in the pre-satellite era is prone to large

1 28 uncertainties. More recent estimates, post IPCC Fourth Assessment report, display a wider
2
3 29 range, between 1.1 and 2. mm/year, based on long-tide-gauges records and estimation of the
4
5 30 Glacial Isostatic Adjustment (Church and White, 2011; Jevrejeva et al. 2014; Hay et al. 2015;
6
7 31 Dangendorf et al., 2017). Very recent estimates resolved at the level of individual ocean basins
8
9 32 (Frederikse et al, 2018), confirm the global figure of 1.5 mm/year (+- 0.2 mm/year) and
10
11 33 indicate a rather strong contribution of the South Atlantic, with 2.56 mm/year (+- 0.47
12
13 34 mm/year) and a very strong acceleration of the South Atlantic sea-level rise over the last 50
14
15 35 years at 0.08 mm/year². Since these results corresponding to the South Atlantic are based on
16
17 36 extrapolation of about 10 records with variable record length, it becomes important to try to
18
19 37 analyze the scarce available information of sea-level rise in the South Atlantic and investigate
20
21 38 the links between sea-level variability in this region and the large-scale climate variability
22
23 39 patterns.
24
25
26
27
28
29
30

31
32 41 The physical mechanism that is behind the sea-level rise are different at the global scale, on
33
34 42 the one hand, and at regional and local scales, on the other hand. (Stammer et al. 2013;
35
36 43 Cazenave and Llovel 2010). Whereas the global mean sea-level is mainly affected by the
37
38 44 thermal expansion of the water column and the melting of land-ice - with more recent
39
40 45 contributions from hydrologic reservoirs and groundwater usage, sea-level rise (SLR)
41
42 46 variations across regional and local scales are also affected by the regionally heterogenous
43
44 47 steric effects (changes in the density structure of the water column associated with temperature
45
46 48 and salinity variations), by the spatially heterogeneous imprint of eustatic effects due to land-
47
48 49 ice melt, and by the effects of regional changes in ocean currents, wind-induced redistributions
49
50 50 of upper-ocean (Figure 1), all of which determine particular spatial characteristics of regional
51
52 51 SLR (Figure 2; Timmermann et al. 2010), and sea-surface topography (Zhang et. al. 2016).
53
54
55
56
57
58
59
60

61 **Figure 1:** Schematic representation of processes that influence sea-level on global to local
62
63 54 scales, (derived from www.nap.edu/read/13389/chapter/3#14)
64
65

55

56 **Figure 2:** Map of global sea-level trends derived from satellite altimetry (Topex Poseidon,
57 Jason-I and Jason-II missions). The focus area of the analysis of this study is indicated by
58 the magenta box (source: <https://image.slidesharecdn.com/observingsealevel29112012-121203090902-phpapp02/95/observing-sea-level-16-638.jpg?cb=1354526006>)

60

61

62 Ghana is the only country in the West African region with tide gauge data dating back to 1929,
63 but there is concern about the data reliability (Woodworth et. al., 2007). Lack of reliable
64 historical sea-level records and research on the influence of large-scale climate impacts on
65 sea-level variability and trends for the GoG limits estimation of sea-level trends and forecast
66 for the region and thus makes coastal communities within the region to be at risk of SLR. It is
67 thus important to improve the accuracy of historical sea-level data for Ghana that can enhance
68 the understanding of climate influence on sea-level trend along the West Africa Coast. Tano
69 et al. (2016) based on 23-year satellite altimeter data reported that relative sea-level has
70 increased around 3.05 mm/y in the GoG.

71

72 Natural climate variability is identified to be important for these sea-level variations across
73 regional ocean basins. The influence of natural climate variability on sea-level patterns and
74 trends has attracted considerable attention during the last decades (Wang and Zhang, 2013;
75 Dangendorf et al. 2014; Tsimplis and Josey, 2001; Woolf et. al., 2003; Wakelin et al., 2003).
76 ENSO, for example, has been identified to influence the regional sea-level variability of the
77 Tropical Pacific (Feng et al., 2015) and has been identified to control multi-decadal variability
78 in US extreme sea-level records (Wahl and Chambers, 2016). In the Atlantic Ocean, the
79 Atlantic Multidecadal Oscillation (AMO) has been identified as an important factor of global
80 and multi-decadal climate variability with the possible influence of natural climate variability

1 81 in the subtropics (Chylek et al., 2014). We will explore in our analysis the link between the
2
3 82 AMO and sea-level in the GoG.

4
5 83

6
7 84 Although there is debate over its region of influence, one widely referenced definition is the
8
9
10 85 revised AMO index by Trenberth and Shea (2006) (Karl et. al. 2009; Coumou et. al. 2013;
11
12 86 Trenberth and Fasullo, 2012; Sung et al., 2015). Trenberth and Shea (2006) defined the AMO
13
14 87 index as the annual mean Sea Surface Temperature (SST) averaged over the region from the
15
16 88 equator (EQ)-60°N, 0°-80°W after subtracting the global mean of SST 60°S-60°N to obtain a
17
18 89 measure of the Atlantic variability that is presumably not related to the external climate
19
20 90 forcing, which would be rather reflected in the global mean SST.
21
22
23
24

25 91

26
27 92 This observed multi-decadal (of the order of magnitude of several decades) variability has a
28
29 93 quasi-periodicity of about 60 to 80 years (Trenberth and Shea 2006), although this difficult to
30
31 94 ascertain due to the limited length of the observational period. The physical origin of the AMO
32
33 95 and its main periodicities are still a matter of debate (see e.g. Booth et al., 2012; Clement et
34
35 96 al.,2015; Wang et al, 2017).
36
37
38
39

40 97

41
42 98 The physical mechanisms that give rise to the AMO are not yet well established. Some studies
43
44 99 have stressed the role of external climate forcing, and of anthropogenic tropospheric aerosols
45
46 100 in the North Atlantic region (Booth et al. 2012). According to this point of view, the AMO
47
48 101 would not as such exist prior to the industrial period, at least not with the presently observed
49
50 102 amplitude. Other studies, on the other hand, have identified purely natural mechanisms that
51
52 103 are capable of inducing oscillation in the North Atlantic SST field (Gastineau and Frankignoul
53
54 104 2015).
55
56
57
58

59 105

60
61 106 From the analysis of simulations with climate models, one theory states that changes in the
62
63 107 salt content influence the ocean circulation in the North Atlantic Ocean (NAO) which in the
64
65

1
2
3
4
5
6
7
8
9
10
11
12
13
14
15
16
17
18
19
20
21
22
23
24
25
26
27
28
29
30
31
32
33
34
35
36
37
38
39
40
41
42
43
44
45
46
47
48
49
50
51
52
53
54
55
56
57
58
59
60
61
62
63
64
65

108 turn changes the NAO thermohaline circulation (THC) resulting in the observed oscillation
109 (Clement et al. 2015). The periodicity of peaks can thus be influenced by the additional
110 freshwater inflow into the NAO (e.g., as a result of gulf-stream and ice-melt). Another theory
111 (Clement et al. 2015) underlines the role of atmospheric variability in the AMO. These authors
112 found that an atmospheric model coupled to a slab ocean model with no ocean dynamics could
113 produce AMO-like variability with AMO being just a thermodynamic response of the ocean
114 mixed layer to stochastic atmospheric forcing. This claim was put into question by Zhang et.
115 al. 2016 who argued that the mechanism causing the AMO in coupled general circulation
116 models is different from that depicted in the slab ocean model used by Clement et al (2015).

117

118 Although confidence in the observational analysis of the AMO is limited by its relatively short
119 instrumental climate record, evidence of long-term internal climate variability over 1400 year
120 control simulation of the Hadley Centre coupled model (HadCM3; Knight et al. 2006), and
121 Coupled Model Intercomparison Project Phase 3 (CMIP3) simulations for the 20th, 21st, and
122 pre-industrial eras (Ting et al. 2011) confirms the effect of AMO on prominent regional
123 climate variability within the northern hemisphere such as Eastern Brazilian and African Sahel
124 rainfall, Atlantic hurricanes and North American and European summer climate (Knight et al.
125 2006; Ting et al. 2011).

126

127 Timmermann et al. (2010), also found wind-induced negative sea-level changes projected for
128 the next 100 years to be quite considerable for many low-lying Pacific Islands which were
129 relatively small (10 - 30%) compared to recent global mean SLR estimates.

130

131

132

1 133 The trends along the West African coast can also be compared to each other and to the
2
3 134 extracted dominant EOFs for the GoG region to determine how the trends are being impacted
4
5 135 by the identified climate variables.
6

7
8 136 Although SLR will likely impact negatively on developing countries including West African
9
10 137 countries (Dasgupta et al. 2007), there exists a lack of information on the impact of large-scale
11
12 138 climate patterns that influence sea-level variability and trends in the (GoG), especially along
13
14 139 the West African coast. The importance of sea-level variability, as well as climate impact
15
16 140 information, was highlighted in a proposed coastal adaptation framework that shows the steps
17
18 141 involved in planned adaptation to climate variability and change by Klein et al., 2006. There
19
20 142 is available literature on coastal impacts and awareness of climate change in Ghana (Evadzi
21
22 143 et al., 2017(a); Evadzi et al., 2017(b); Jayson-Quashigah et al., 2013; Appeaning Addo 2008,
23
24 144 2011 and 2013; Amlalo, 2006).
25
26
27
28

29 145 In summary, an assessment of the large-scale climate forcing that drives sea-level variability
30
31 146 in the GoG with more focus on the West African coast was performed. Attempts to reconstruct
32
33 147 observed instrumental sea-level data for Ghana to improve its accuracy and explains the
34
35 148 decadal variability were also made. In the following, we specify the methodology and present
36
37 149 the results.
38
39
40
41

42 150

43 44 151 **METHODS**

45
46
47 152 The methods section comprises two parts: the first part describes the study area while the
48
49 153 second presents the data and processing methods used for the data analysis.
50
51

52 154

53 54 155 **Study Area**

55
56
57
58 156 Our study area is the Gulf of Guinea, defined here as the region in the geographical box
59
60 157 displayed in Figure 3. This region is selected to take into account the relatively coarse
61
62 158 resolution of simulations with climate models and satellite altimetry data. Within this region,
63
64
65 159 there are only few relatively long-tide-gauge records from the Permanent Service for Mean

160 Sea-level (PSMSL), (Takoradi and Tema (Ghana) and Forcados (Nigeria) located on the coast
 161 of West Africa. The Forcados tide-gauge station although with fewer records, is assumed to
 162 be reasonably accurate based on data assessment by the PSMSL. The large-scale region in
 163 which the connections to GoG sea-level will be sought is defined here as the broad Tropical
 164 Atlantic region within the geographical box 80W° to 40E° and latitudes 40S° to 40N°. In this
 165 region, monthly-mean sea-surface heights (SSH) data from satellite observations and ocean
 166 models, wind stress data from meteorological reanalysis and sea-surface temperature were
 167 extracted as described below and summarised in Table 1.

168

169 Figure 3: Study area showing the Gulf of Guinea and selected tide gauge stations [Takoradi
 170 and Tema (Ghana) and Forcados (Nigeria)] along the West Africa coast

171

172 **Data and methods**

173 Our objective is to identify the large-scale drivers of sea-level variability at monthly time
 174 scales, and their trends, in the GoG. The observational basis is limited to the tide-gauge
 175 records of Takoradi and Tema. The Takoradi station reports data from 1929 onwards.
 176 However, these data have been labelled as unreliable after 1966. The Tema record covers the
 177 period 1963-1982. This record is, in contrast, deemed as accurate by the Permanent Service
 178 for Mean Sea-level. We first try to construct a synthetic Takoradi record using the data from
 179 these two tide-gauges, based on their mutual correlation during the overlapping period (1963-
 180 1965). The uncertainties in the Takoradi record are related to its long-term trends after and
 181 therefore, we first compute a high-pass filtered version of both records to correlate their
 182 monthly variations (Equation 1):

183

184 (i) $[Tema-Tema^{1963-1965}] \propto [Takoradi-Takoradi^{1963-1965}]$
 185 (ii) $Takoradi_t = \alpha \cdot [Tema_t - Tema_t^{1963-1965}] + [Takoradi_t^{1963-1965}]$ (Equation 1)

186 In this equation

187 (i) represents the correlation for the overlap period

188 (ii) represents the estimation rule, and

189 $\alpha =$ correlating the overlap period of Takoradi t and Tema t , $t = 1963-1965$

190

191 Equation (1) provides a synthetic record at Takoradi using the information included in the
192 Tema record. Therefore, this record can be considered as a regional sea-level curve for Ghana,
193 covering five decades (1929-1981; Figure 4). The increased length of this synthetic record
194 will increase the robustness of the following statistical analysis that aims to identify the large-
195 scale climate patterns that are closely linked to sea-level in the GoG. We also statistically
196 explore the connections between sea-level variability in the GoG with sea-level recorded in
197 the neighbouring Nigeria records.

198

199 **Figure 4:** Reconstructed Ghana Annual Mean Sea-level (AMSL) curve together with Ghana
200 tide gauge record Takoradi (from PSMSL, not reliable after 1966)

201

202 Statistical analysis of the sea-level pattern in the GoG by means of Empirical Orthogonal
203 Function (EOF) and assessment of the impact of AMO on observed sea-level record for the
204 region was performed. The EOF analysis, also referred to as Principal Component Analysis
205 (PCA), is a multivariate statistical method that serves as a means of extracting the dominant
206 patterns from data sets and has been widely utilized in sea-level variability analysis (Church
207 et al. 2004; Cheng et al. 2015; Hay et al. 2015).

208

209 EOF analysis was applied to the satellite sea-level data to first identify the main patterns of
210 large-scale sea-level variability. In this analysis, SSH data from the combined satellite
211 missions TOPEX/Poseidon, Jason-1, and Jason-2/OSTM were included. These data have been

1
2
3
4
5
6
7
8
9
10
11
12
13
14
15
16
17
18
19
20
21
22
23
24
25
26
27
28
29
30
31
32
33
34
35
36
37
38
39
40
41
42
43
44
45
46
47
48
49
50
51
52
53
54
55
56
57
58
59
60
61
62
63
64
65

212 previously widely used for sea-level analysis (Han et al. 2014; Lyu et al. 2014). There are
213 different versions of these data sets depending on the different corrections included. These
214 corrections may refer to the inverse barometer effect (the effect of air pressure on SSH) also
215 the annual and semi-annual cycles. For the present analysis, we did not choose the data version
216 corrected for the Glacial Isostatic Adjustment (GIA). The GIA is caused by the remnant
217 viscous readjustment of the Earth crust to the ice load and its sequent demise, of the large
218 continental ice sheets of the Northern hemisphere during the last glacial age that terminated
219 about 10 000 years ago. This correction is very small in the GoG. An additional reason is that
220 the tide-gauge data, with which we would also compare the satellite products, are not corrected
221 for the GIA.

222

223 The results of the EOF analysis on the satellite altimetry data was compared with a similar
224 analysis on two other data sets. One is the output of an ocean simulation with the model MPIO-
225 OM of the Max-Planck-Institute of Meteorology in Hamburg. This simulation, hereafter
226 referred to as the STORM simulation (Storch et al., 2012), has a horizontal resolution of about
227 10 km, and therefore the global ocean is very highly resolved. The atmospheric data used to
228 drive the ocean model were from the meteorological reanalysis of the National Center for
229 Environmental Prediction and the National Center for Atmospheric Research. These data are
230 referred to as the NCEP/NCAR reanalysis (Kistler et al. 2001). They cover the period 1948
231 until today, although the ocean simulation here stops in the year 2010.

232 The atmospheric data reproduce the observed weather sequence over the last decades, and
233 thus the output of the ocean simulation can be compared with observational data sets, with
234 one limitation. This limitation is the contribution to sea-level rise by the melting of continental
235 land-ice. This contribution is not included in the STORM simulation and therefore, the
236 simulated long-term trends, which include only other factors like the thermal expansion of the
237 water column or the impact of wind-stress on the ocean surface, will generally be smaller than
238 the observed long term sea-level trends.

1
2
3
4
5
6
7
8
9
10
11
12
13
14
15
16
17
18
19
20
21
22
23
24
25
26
27
28
29
30
31
32
33
34
35
36
37
38
39
40
41
42
43
44
45
46
47
48
49
50
51
52
53
54
55
56
57
58
59
60
61
62
63
64
65

239 Other than this, the NCEP/NCAR reanalysis results from the combination (data assimilation)
240 of a huge set of observations, from multiple sources such as station data, satellite data, ships
241 observations, etc, with a numerical weather prediction model. The weather trajectories
242 simulated by this model are readjusted within a data assimilation scheme to resemble as close
243 as possible the set of observations available. The resulting model output covers a three-
244 dimensional global grid of 2.5 x 2.5 (Lon. x Lat.) horizontal resolution. The wind stress data
245 also stem from the NCAR/NCEP reanalysis

246

247 We also use the observationally-based gridded reconstruction of SSH in the period 1950-2001
248 by Church et al. (2004). The reconstructions are based on a statistical analysis of a set of tide-
249 gauge monthly records, combined with the main patterns of variability derived from an EOFs
250 analysis of the satellite altimetry fields TOPEX/Poseidon + Jason-1.

251 The reconstruction process is based on the identification of the spatially resolved leading
252 patterns of sea-level variability at global scales in the satellite era by means of an EOF
253 analysis. The time-varying amplitude of these EOF patterns (their associated principal
254 components) in the pre-satellite era is estimated from the available tide-gauge data, by fitting
255 the tide-gauge sea-level anomalies to the EOF patterns. This yields a spatially resolved sea-
256 level reconstruction. The level of spatial detail and resolution of this reconstruction is limited
257 by the spatial structures of the retained EOF patterns (Church et al., 2004).

258

259 The gridded observations of SST used here stem from the Hadley Centre Sea Ice and Sea
260 Surface Temperature dataset (HadISST, version 1). The data are a result of an optimal
261 interpolation of available ships observations. This data set has found many other applications
262 in climate studies (Feng et al. 2015; Harlass et. al. 2015).

263

264

265

266 The link between sea-level in the GoG and the large-scale climate information is conducted

1 267 by statistical analysis of the long-term de-trended annual means for all dataset. This procedure
2
3 268 avoids the identification of artefact correlations simply due to the presence of long-term trends
4
5 269 in the data sets. It also filters out long-term trends in sea-level caused by the long-term
6
7 270 warming of the oceans and melting of land-ice that is not reflected in trends of the other
8
9 271 climate parameters, like wind stress. (Wu et al. 2007).

12
13 **Table 1:** Data used in this study with a summary description of their spatial resolution
14
15

16 273

19 274 RESULTS

20
21
22 275 The results section covers two main topics: sea-level variability and impact of large-scale
23
24 276 climate patterns on sea-level variations.

25
26
27 277 We address here two aspects: sea variability in the GoG and the influence of the large-scale
28
29 278 climate patterns on sea-level in the GoG.

31 279 **Sea-level Variability**

32
33
34
35
36 280 The identification of the leading patterns of sea-level variability in the GoG was achieved by
37
38 281 an EOF analysis. This analysis was conducted on normalized sea-level records (each grid-cell
39
40 282 record normalized to unit variance) for the satellite, MPI-OM, and Church et al (2004)
41
42 283 reconstruction SSH datasets (Figure 5). This normalization is required since the different data
43
44 284 sets may display different levels of variability. The scale bar for Figure 5 only depicts the
45
46 285 normalized range with dimensionless values. The leading normalized EOF patterns of SSH-
47
48 286 derived from Satellite-SSH (Figure 5a) and MPI-OM-SSH (Figure 5b) show similar patterns
49
50 287 in the tropics, but opposite patterns in the extra-tropics. Both explain about 20% of the
51
52 288 variability and their spatial patterns are reasonably similar. In contrast, the leading EOF
53
54 289 pattern derived from Church-SSH (Figure 5c) displays a uniform sign for the whole region
55
56 290 and explains 48% of the variance. The reason for this discrepancy might lie in the
57
58 291 reconstruction method. Since the reconstruction method applied by Church et al., already
59
60 292 incorporates a prefiltering of the small-scale patterns of variability, it is logical that the leading
61
62
63
64
65

1
2
3
4
5
6
7
8
9
10
11
12
13
14
15
16
17
18
19
20
21
22
23
24
25
26
27
28
29
30
31
32
33
34
35
36
37
38
39
40
41
42
43
44
45
46
47
48
49
50
51
52
53
54
55
56
57
58
59
60
61
62
63
64
65

293 EOF patterns of this data sets can already explain a larger part of the total variability of the
294 Church et al. (2004) data sets. The results suggest that the Church et al. (2004) SSH
295 reconstruction is not able to capture smaller-scale regional to local patterns in our region of
296 interest (refer to Table 2 for the percentage of variance for the 4 leading EOFs of the datasets).

297

a) Satellite-SSH normalized EOF1 (1993-2013) 20.22% explained variance *b) MPI-OM normalized EOF1 (1990-2010) 19.54% explained variance*

300

301

302

c) Church rec. normalized EOF1 (1950-2001) 48.63 % explained variance

303

304

305 **Figure 5:** Normalized patterns of leading Empirical Orthogonal Functions of the annual
306 mean sea-surface height (de-trended) for different datasets: **a)** satellite data, **b)** ocean-only
307 simulation from MPI-OM and **c)** reconstructed SSH from Church et al. 2004

308

309 **Table 2:** The percentage of the variance of the 4 leading EOFs of the annual mean SSH and
310 SST from the different sources used in this study data sets

311

312 **Impact of large-scale climate patterns**

313 The large-scale sea-level patterns of variability were identified by means of EOF analysis. For
314 this analysis, the SSH and the SST data were not normalized (not reduced to unit standard
315 deviation) in each grid-cell of the corresponding data set to obtain an estimation of the real
316 amplitude of this variability (Fig 7a and Fig 7b)

317

318 The leading EOF patterns of SST (Figure 7a) show higher values in the tropics and opposite
319 anomalies in the extra-tropics. The study finds a positive correlation ($r = 0.32$) between the

1 320 time-series (principal components) of the leading EOFs of satellite-SSH and the SST (Figure
2
3 321 6). From these two spatial patterns, we can roughly estimate if the link between these two
4
5 322 patterns are physically plausible We can and estimate the thermosteric expansion effect of ~
6
7 323 0.8 Kelvin, which is the average value of the SST EOF1 for Ghana, Figure 7a) To estimate
8
9 324 the magnitude of the thermal expansion, we assume that the temperature anomalies at the
10
11 325 surface are representative of the upper 50 meters of coastal seawater column and have an
12
13 326 average salinity of about 30 psu. We also neglect in this calculation any spill-over effect of
14
15 327 the thermal expansion of the water column in the open ocean towards more shallow coastal
16
17 328 areas. Based on a thermal expansion coefficient of $250 \times 10^{-6} /K$, a one K warming of the
18
19 329 upper 50 meters should result in an expansion of the water column of 12.5 mm.
20
21
22
23
24
25
26
27

28 331 **Figure 6:** Time series of AMO index (blue), principal component 1 Satellite-SSH (red) and
29
30 332 principal component 1 of SST (green) for the period 1993-2013
31
32

33 333

34
35 334 We now turn our attention to investigate the links between sea-level variability in the GoG
36
37 335 and the Atlantic Multidecadal Oscillation (AMO). The AMO has been described as the
38
39 336 multidecadal variability of the sea-surface temperatures in the North Atlantic (Chylek et al.
40
41 337 2014). It has been identified as an important climate driver in this region. We explore the link
42
43 338 between the AMO and sea-level in the GoG by calculating the correlation between the AMO
44
45 339 index and the SST and SSH in the GoG. (Figure 8).
46
47
48
49

50 340

51 341

52 342

(a)

(b)

53 343

54
55 344 **Figure 7:** Pattern of leading Empirical Orthogonal Functions of the annual mean sea-

56
57 345 surface-temperature from HadISST and satellite-SSH. **a)** *HadISST1 EOF1 (1993-2013)*

58
59 346 *27.34% explained variance; b)* *Satellite-SSH EOF1 (1993-2013) 20.22% explained variance*
60
61
62
63
64
65

1 347

2
3
4 348 The AMO index has also been correlated with the reconstructed SSH record at Takoradi and
5
6 349 at the tide-gauge of Forkados in Nigeria (Figure 9). The purpose of this analysis is to establish
7
8 350 to what extent the connection between the AMO and West Africa sea-level can be reproduced
9
10
11 351 in the satellite data and in the tide-gauge data.

12
13
14 352

15
16
17
18 353 **Figure 8:** Correlation pattern between the AMO index and the annual mean SSH from
19
20 354 satellite altimetry

21
22 355

23
24
25
26 356 **Figure 9:** Time series of the AMO index together with tide gauge record of Forcado/
27
28 357 Nigeria and the Ghana annual mean sea-level reconstruction

29
30 358

31
32
33 359 This analysis (Figure 8) shows relatively strong correlations between AMO and sea-level in
34
35 360 the whole Tropical Atlantic, but the impact of AMO on sea-level seems to be larger along the
36
37 361 West African coast. However, the pattern along the West African coast varies. For example,
38
39 362 the correlation between AMO and SSH on the Ghana coast is stronger than at the Nigeria
40
41 363 coast. The evidence of this AMO impact on sea-level variability at the West Africa coast is
42
43 364 reflected in the decadal variations of AMO and the decadal variations of time series of the
44
45 365 reconstructed Ghana AMSL and that of Nigeria (Figure 9) although the available data for
46
47 366 Nigeria is inadequate for long term analysis. The agreement between the AMO index and the
48
49 367 reconstructed Ghana sea-level record is poorer in the early parts of the record, before 1940,
50
51 368 but it is much better thereafter. It shows a maximum of the AMO and of sea-level at around
52
53 369 1955, with declining values thereafter until around 1975. In the subsequent years, both indices
54
55 370 of the AMO and of the reconstructed Ghana sea-level recover towards more positive values.
56
57 371 Since the AMO and satellite-SSH were found to be positively correlated, the agreement in the
58
59 372 long-term AMO and SSH indices support the robustness of the Ghana SSH reconstructions

1 373 despite the cautions that should be placed on the Ghana tide-gauge records.
2
3

4 374

5
6 375 Regarding the effect of winds on sea-level variability in the GoG, although the wind has been
7
8
9 376 hinted at as an important driver of sea-level variability (Thompson et al. 2014; Timmermann
10
11 377 et. al. 2010), our statistical analysis did not find a clear connection between wind-stress and
12
13 378 sea-level variations in the GoG.
14
15

16
17 379

18
19 380

20 21 381 **DISCUSSION**

22
23 382

24
25 383 Large-scale climate patterns are identified to impact regional sea-level variability at various
26
27 384 locations globally which in turn could affect coastlands at different rates. Although Chylek et
28
29 385 al. 2014 identified AMO to have a possible influence of natural climate variability in the
30
31 386 subtropics there are different theories that attempt to explain the mechanism AMO.
32
33

34
35 387

36
37 388 With regards to sea-level change on West Africa, Tano et al. 2016 based on 23-year satellite
38
39 389 altimeter data reported that relative sea-level has increased around 3.05 mm/y in the GoG.
40
41 390 Evadzi et. al. 2017(a), estimated that computed sea-level trend from satellite-SSH data (1993-
42
43 391 2013) at the coast of Ghana (2.52 ± 0.22 mm/y), contributed to ~ 31 % of observed historical
44
45 392 shoreline change (~ 2 m/y) for the coast of Ghana from 1974 to 2015.
46
47
48

49 393

50
51 394 The SST variations are found to be associated with sea-level variability in the GoG since
52
53 395 normalized leading EOF(s) patterns from satellite-SSH (1993-2013) and SST show similar
54
55 396 spatial structure in the tropics and opposite patterns in the extra-tropics. The positive
56
57 397 correlation found between the principal components of the leading EOFs of SSH and SST
58
59 398 allows for an estimation of the thermosteric effect on sea-level variability, under some
60
61 399 reasonable physical conditions (SST sharing the warming/cooling with the upper 50 meters of
62
63
64
65

1 400 the water column and constant salinity at 30 psu), yielding an amplitude of SSH variability in
2
3 401 the GoG of 1 mm per 0.8 K of SST variability.

4
5 402

6
7 403 The AMO is found to be more strongly correlated with SSH at the coast of Ghana than in
8
9 404 Nigeria (Fig. 8). In addition, the long-term trend of the AMO also influences the long term
10
11 405 trend of Ghana and Nigeria SSH. (Figure 9). The agreement between the AMO indices and
12
13 406 the reconstructed Ghana SSH gives more credibility to the Ghana tide-gauge records, at least
14
15 407 in their multidecadal variations. In particular, the declining sea-level at the Ghana coast in the
16
17 408 period between 1955 and 1975 approximately is as reflected in similar variations of the AMO
18
19 409 index. The connection between AMO and SSH in the Tropical Atlantic is also supported by
20
21 410 the found correlations with satellite altimetry in the satellite era, Therefore, the common
22
23 411 evolution of the AMO and Ghana SSH at decadal time scales in the pre-satellite era seems to
24
25 412 be physically supported.

26
27 413

28
29 414

30
31 415

32 **CONCLUSIONS**

33
34 416 Although there exists literature on sea-level impact on the coast of Ghana there is lack of
35
36 417 information on sea-level variability and trends for Ghana and the entire Gulf of Guinea
37
38 418 region. This study attempts to provide this information that may be useful for adaptation
39
40 419 strategies.

41
42 420 There are several factors that are identified in this statistical analysis as drivers of SSH
43
44 421 variability in the GoG. One is sea-surface-temperature. In addition, the Atlantic
45
46 422 Multidecadal Oscillation displays a clear link to SSH variability in this region, in both
47
48 423 satellite altimetry data and in tide-gauge data from Ghana and Nigeria. In contrast, no
49
50 424 statistical influence by the wind -stress on SSH variability in the GoG could be identified in
51
52 425 this study.

1 426 Although this study reconstructed regional mean sea-level curve for Ghana, there exist no
2
3 427 data for the period from 1981 to 1993 between the reconstructed regional sea-level curve for
4
5 428 Ghana and existing satellite altimetry data on sea-level change for the Gulf of Guinea for
6
7 429 detail analysis on sea-level trend for Ghana. Such research will be useful for forecast and
8
9
10 430 improve coastal adaptation strategies.
11

12
13 431

17 432 REFERENCES

18
19 433

20
21
22 434 Amlalo DS (2006) The protection, management and development of the marine and coastal
23
24 435 environment of Ghana. *Administering marine spaces*, International issues. International
25
26 436 Federation of Surveyors, Copenhagen, Denmark

27 437 Anthoff D, Nicholls RJ, Tol RS, and Vafeidis AT (2006) Global and regional exposure to
28
29 438 large rises in sea-level: a sensitivity analysis. Tyndall centre for climate change
30
31 439 research-Working Paper, 96

32
33 440 Appeaning Addo K (2011) Changing morphology of Ghana's Accra coast. *Journal of*
34
35 441 *Coastal Conservation* 15(4): 433–443. doi:10.1007/s11852-010-0134-z

36 442 Appeaning Addo K (2013) Assessing coastal vulnerability index to climate change: The case
37
38 443 of Accra-Ghana. In: Conley D; Masselink G; Russell P, and O'Hare T (eds.)
39
40 444 Proceedings from the International Coastal Symposium (ICS) (2013) Volume 1. *Journal*
41
42 445 *of Coastal Research*, Special Issue No. 65: 1892–1897.

43 446 Appeaning Addo K, Walkden M, and Mills JP (2008) Detection, measurement and
44
45 447 prediction of shoreline recession in Accra, Ghana. *ISPRS Journal of Photogrammetry*
46
47 448 *and Remote Sensing* 63(5): 543–558. doi:10.1016/j.isprsjprs.2008.04.001

48
49 449 Booth BB, Dunstone NJ, Halloran PR, Andrews T, Bellouin N (2012) Aerosols implicated
50
51 450 as a prime driver of twentieth-century North Atlantic climate variability. *Nature*
52
53 451 484(7393): 228-232

54 452 Cazenave A, Llovel W (2010) Contemporary sea-level rise. *Ann Rev Mar Sci* 2:145–173.
55
56 453 doi: 10.1146/annurev-marine-120308-081105

57
58 454 Cheng Y, Plag H-P, Hamlington BD, Xu Q, He Y (2015) Regional sea-level variability in
59
60 455 the Bohai Sea, Yellow Sea, and East China Sea. *Continental Shelf Research* 111:95–
61
62 456 107. doi: 10.1016/j.csr.2015.11.005
63
64
65

1 457 Church JA, Clark PU, Cazenave A, Gregory JM, Jevrejeva S, Levermann A, Merrifield MA,
2 458 Milne GA, Nerem RS, Nunn PD, Payne AJ, Pfeffer WT, Stammer D, Unnikrishnan AS
3
4 459 (2013) Sea level change. In: Stocker TF, Qin D, Plattner G-K, Tignor M, Allen SK,
5
6 460 Boschung J, Nauels A, Xia Y, Bex V, Midgley PM (eds.), Climate Change (2013): The
7
8 461 Physical Science Basis. Contribution of Working Group I to the Fifth Assessment
9
10 462 Report of the Intergovernmental Panel on Climate Change. New York: Cambridge
11
12 463 University Press, 79

13 464 Church JA, White NJ, Coleman R, Lambeck K, Mitrovica JX (2004) Estimates of the
14
15 465 Regional Distribution of Sea-level Rise over the 1950–2000 Period. *J. Climate*
16
17 466 17(13):2609–2625. doi: 10.1175/1520-0442(2004)017<2609:EOTRDO>2.0.CO;2

18 467 Church, J. A. and White, N. J. (2011). Sea-level rise from the late 19th to the early 21st
19
20 468 century. *Surveys in geophysics*, 32(4-5), 585-602. doi:10.1007/s10712-011-9119-1

21 469 Chylek P, Klett JD, Lesins G, Dubey MK, Hengartner N (2014) The Atlantic Multidecadal
22
23 470 Oscillation as a dominant factor of oceanic influence on climate. *Geophys. Res. Lett.*
24
25 471 41(5):1689–1697. doi: 10.1002/2014GL059274

26 472 Coumou D, Robinson A, Rahmstorf S (2013) Global increase in record-breaking monthly-
27
28 473 mean temperatures. *Climatic Change* 118(3-4):771–782. doi: 10.1007/s10584-012-0668-
29
30 474 1

31 475 Dangendorf S, Rybski D, Mudersbach C, Müller A, Kaufmann E, Zorita E, Jensen J (2014)
32
33 476 Evidence for long-term memory in sea-level. *Geophys. Res. Lett.* 41(15):5530–5537.
34
35 477 doi: 10.1002/2014GL060538

36 478 Dangendorf, S., Marcos, M., Wöppelmann, G., Conrad, C. P., Frederikse, T., & Riva, R.
37
38 479 (2017). Reassessment of 20th century global mean sea-level rise. *Proceedings of the*
39
40 480 *National Academy of Sciences*, 114(23), 5946-5951. doi:10.1073/pnas.1616007114

41 481 Dasgupta S, Laplante B, Meisner C, Wheeler D, Yan J (2007) The Impact of Sea-level Rise
42
43 482 on Developing Countries: A Comparative Analysis.
44
45 483 <https://openknowledge.worldbank.org/bitstream/10986/7174/1/wps4136.pdf>

46 484 Evadzi P, Zorita E, Hünicke B (2017 (a)) Quantifying and predicting the contribution of sea-
47
48 485 level rise to shoreline change in Ghana: Information for coastal adaptation strategies.
49
50 486 *Journal of Coastal Research*, (In-Press. <https://doi.org/10.2112/JCOASTRES-D-16-00119.1>)

51 487
52 488 Evadzi P, Zorita E, Hünicke B (2017 (b)) Awareness of sea-level response under climate
53
54 489 change on the coast of Ghana. *Journal of Coastal Conservation* (Accepted and In-
55
56 490 Production DOI: 10.1007/s11852-017-0569-6)

1
2
3
4
5
6
7
8
9
10
11
12
13
14
15
16
17
18
19
20
21
22
23
24
25
26
27
28
29
30
31
32
33
34
35
36
37
38
39
40
41
42
43
44
45
46
47
48
49
50
51
52
53
54
55
56
57
58
59
60
61
62
63
64
65

491 Feng M, Hendon HH, Xie S-P, Marshall AG, Schiller A, Kosaka Y, Caputi N, Pearce A
492 (2015) Decadal increase in Ningaloo Niño since the late 1990s. *Geophys. Res. Lett.*
493 42(1):104–112. doi: 10.1002/2014GL062509

494 Frederikse, T., Jevrejeva, S., Riva, R. E., & Dangendorf, S. (2018). A consistent sea-level
495 reconstruction and its budget on basin and global scales over 1958–2014. *Journal of*
496 *Climate*, 31(3), 1267-1280. doi: 10.1175/JCLI-D-17-0502.1

497 Gastineau G, Frankignoul C (2015) Influence of the North Atlantic SST Variability on the
498 Atmospheric Circulation during the Twentieth Century. *J. Climate* 28(4):1396–1416.
499 doi: 10.1175/JCLI-D-14-00424.1

500 Han G, Ma Z, Bao H, Slangen A (2014) Regional differences of relative sea-level changes in
501 the Northwest Atlantic: Historical trends and future projections. *J. Geophys. Res.*
502 *Oceans* 119(1):156–164. doi: 10.1002/2013JC009454

503 Harlaß J, Latif M, Park W (2015) Improving climate model simulation of tropical Atlantic
504 sea surface temperature: The importance of enhanced vertical atmosphere model
505 resolution. *Geophys. Res. Lett.* 42(7):2401–2408. doi: 10.1002/2015GL063310

506 Hay CC, Morrow E, Kopp RE, Mitrovica JX (2015) Probabilistic reanalysis of twentieth-
507 century sea-level rise. *Nature* 517(7535):481–484. doi: 10.1038/nature14093

508 IPCC (Intergovernmental Panel on Climate Change) (2013) The Physical Science Basis.
509 WGI AR5. Technical report. <http://www.ipcc.ch/report/ar5/wg1/>

510 Jayson-Quashigah P-N, Appeaning Addo K, Kufogbe SK (2013) Medium resolution satellite
511 imagery as a tool for monitoring shoreline change. Case study of the Eastern coast of
512 Ghana. *Journal of Coastal Research*, Special Issue No. 65: 511–516. doi:10.2112/SI65-
513 087.1

514 Jevrejeva, S., Moore, J. C., Grinsted, A., Matthews, A. P., & Spada, G. (2014). Trends and
515 acceleration in global and regional sea-level s since 1807. *Global and Planetary Change*,
516 113, 11-22. doi:10.1016/j.gloplacha.2013.12.004

517 Karl TR, Melillo JM, Peterson TC, Hassol SJ (ed) (2009) Global climate change impacts in
518 the United States: A state of knowledge report from the U.S. Global Change Research
519 Program. Cambridge University Press, Cambridge

520 Klein RJ, Dougherty WW, Alam M, Rahman A (2005). Technology to understand and
521 manage climate risks. *In* Background Paper for the UNFCCC Seminar on the
522 Development and Transfer of Environmentally Sound Technologies for Adaptation to
523 Climate Change, Tobago 2005 Jun (pp. 14-16).

524 Knight JR, Folland CK, Scaife AA (2006) Climate impacts of the Atlantic Multidecadal
525 Oscillation. *Geophys. Res. Lett.* 33(17). doi: 10.1029/2006GL026242

1 526 Lyu K, Zhang X, Church JA, Slangen ABA, Hu J (2014) Time of emergence for regional
2 527 sea-level change. *Nature Climate change* 4(11):1006–1010. doi: 10.1038/nclimate2397
3
4 528 NCEP/NCAR (Accessed 2014) 40-Year Reanalysis Project 77:437–470.
5
6 529 <http://www.esrl.noaa.gov/psd/data/gridded/data.ncep.reanalysis.html>
7
8 530 NOAA (National Oceanic and Atmospheric Administration) (2013) Mean Sea-Level Trends
9
10 531 410-001 Takoradi, Ghana.
11
12 532 https://tidesandcurrents.noaa.gov/sltrends/sltrends_global_station.htm?stnid=410-001
13
14 533 Permanent Service for Mean Sea-level (2014) "Tide Gauge Data" Retrieved 20 July 2014
15 534 from <http://www.psmsl.org/data/obtaining/>
16
17 535 Rayner NA (2003) Global analyses of sea surface temperature, sea ice, and night marine air
18 536 temperature since the late nineteenth century. *J. Geophys. Res.* 108(D14). doi:
19 537 10.1029/2002JD002670
20
21 538 Stammer D, Cazenave A, Ponte RM, Tamisiea ME (2013) Causes for contemporary regional
22 539 sea-level changes. *Ann Rev Mar Sci* 5:21–46. doi: 10.1146/annurev-marine-121211-
23 540 172406
24
25 541 Storch J-Sv, Eden C, Fast I, Haak H, Hernández-Deckers D, Maier-Reimer E, Marotzke J,
26 542 Stammer D (2012) An Estimate of the Lorenz Energy Cycle for the World Ocean Based
27 543 on the STORM/NCEP Simulation. *J. Phys. Oceanogr.* 42(12):2185–2205. doi:
28 544 10.1175/JPO-D-12-079.1
29
30 545 Sung M-K, An S-I, Kim B-M, Kug J-S (2015) Asymmetric impact of Atlantic Multidecadal
31 546 Oscillation on El Niño and La Niña characteristics. *Geophys. Res. Lett.* 42(12):4998–
32 547 5004. doi: 10.1002/2015GL064381
33
34 548 Tano RA, Aman A, Kouadio KY, Toualy E, Ali KE, Assamoi P (2016) Assessment of the
35 549 Ivorian Coastal Vulnerability. *Journal of Coastal Research* 322:1495–1503. doi:
36 550 10.2112/JCOASTRES-D-15-00228.1
37
38 551 Timmermann A, McGregor S, Jin F-F (2010) Wind Effects on Past and Future Regional
39 552 Sea-level Trends in the Southern Indo-Pacific. *J. Climate* 23(16):4429–4437. doi:
40 553 10.1175/2010JCLI3519.1
41
42 554 Ting M, Kushnir Y, Seager R, Li C (2011) Robust features of Atlantic multi-decadal
43 555 variability and its climate impacts. *Geophys. Res. Lett.* 38(17):n/a-n/a. doi:
44 556 10.1029/2011GL048712
45
46 557 Trenberth KE, Fasullo JT (2012) Climate extremes and climate change: The Russian heat
47 558 wave and other climate extremes of 2010. *J. Geophys. Res.* 117(D17). doi:
48 559 10.1029/2012JD018020
49
50 560 Trenberth KE, Shea DJ (2006) Atlantic hurricanes and natural variability in 2005. *Geophys.*
51 561 *Res. Lett.* 33(12). doi: 10.1029/2006GL026894
52
53
54
55
56
57
58
59
60
61
62
63
64
65

1
2
3
4
5
6
7
8
9
10
11
12
13
14
15
16
17
18
19
20
21
22
23
24
25
26
27
28
29
30
31
32
33
34
35
36
37
38
39
40
41
42
43
44
45
46
47
48
49
50
51
52
53
54
55
56
57
58
59
60
61
62
63
64
65

562 Tsimplis MN, Josey SA (2001) Forcing of the Mediterranean Sea by atmospheric
563 oscillations over the North Atlantic. *Geophys. Res. Lett.* 28(5):803–806. doi:
564 10.1029/2000GL012098

565 Wahl T, Chambers DP (2016) Climate controls multidecadal variability in U. S. extreme
566 sea-level records. *J. Geophys. Res. Oceans* 121(2):1274–1290. doi:
567 10.1002/2015JC011057

568 Wakelin SL, Woodworth PL, Flather RA, Williams JA (2003) Sea-level dependence on the
569 NAO over the NW European Continental Shelf. *Geophys. Res. Lett.* 30(7). doi:
570 10.1029/2003GL017041

571 Wang C, Zhang L (2013) Multidecadal Ocean Temperature and Salinity Variability in the
572 Tropical North Atlantic: Linking with the AMO, AMOC, and Subtropical Cell. *J.*
573 *Climate* 26(16):6137–6162. doi: 10.1175/JCLI-D-12-00721.1

574 Woodworth PL, Aman A, Aarup T (2007) Sea-level monitoring in Africa. *African Journal of*
575 *Marine Science* 29(3):321–330. doi: 10.2989/AJMS.2007.29.3.2.332

576 Woolf DK, Shaw AGP, Tsimplis MN (2003) The influence of the North Atlantic Oscillation
577 on sea-level variability in the North Atlantic region. *Journal of Atmospheric & Ocean*
578 *Science* 9(4):145–167. doi: 10.1080/10236730310001633803

579 Wu Z, Huang NE, Long SR, Peng C-K (2007) On the trend, detrending, and variability of
580 nonlinear and nonstationary time series. *Proc Natl Acad Sci U S A* 104(38):14889–
581 14894. doi: 10.1073/pnas.0701020104

582 Zhang J, Kelly KA, Thompson L (2016) The role of heating, winds, and topography on sea-
583 level changes in the North Atlantic. *J. Geophys. Res. Oceans* 121(5):2887–2900. doi:
584 10.1002/2015JC011492

585
586
587

588 **LIST OF FIGURES**

589 Figure 1: Schematic representation of processes that influence sea-level on global to local
590 scales, (derived from www.nap.edu/read/13389/chapter/3#14)

591 Figure 2: Map of global sea-level trends derived from satellite altimetry (Topex Poseidon,
592 Jason-I and Jason-II missions). The focus area of the analysis of this study is
593 indicated by the magenta box

1 594 (source:<https://image.slidesharecdn.com/observingsealevel29112012-121203090902->
2
3 595 [phpp02/95/observing-sea-level-16-638.jpg?cb=1354526006](https://image.slidesharecdn.com/observing-sea-level-16-638.jpg?cb=1354526006)
4

5 596 Figure 3: Study area showing the Gulf of Guinea and selected tide gauge stations [Takoradi
6
7
8 597 and Tema (Ghana) and Forcados (Nigeria)] along the West Africa coast
9

10 598 Figure 4: Reconstructed Ghana Annual Mean Sea-level (AMSL) curve together with Ghana
11
12 599 tide gauge record Takoradi (from PSMSL, not reliable after 1966)
13
14

15 600 Figure 5: Normalized patterns of leading Empirical Orthogonal Functions of the annual
16
17 601 mean sea-surface height (de-trended) for different datasets: a) satellite data, b) ocean-
18
19 602 only simulation from MPI-OM and c) reconstructed SSH from Church et al. 2004
20
21

22 603 Figure 6: Time series of AMO index (blue), principal component 1 Satellite-SSH (red) and
23
24 604 principal component 1 of SST (green) for the period 1993-2013
25
26

27 605 Figure 7: Pattern of leading Empirical Orthogonal Functions of the annual mean sea-surface-
28
29 606 temperature from HadISST and satellite-SSH. a) HadISST1 EOF1 (1993-2013)
30
31 607 27.34% explained variance; b) Satellite-SSH EOF1 (1993-2013) 20.22% explained
32
33 608 variance
34
35
36

37 609 Figure 8: Correlation pattern between the AMO index and the annual mean SSH from
38
39 610 satellite altimetry
40
41

42 611 Figure 9: Time series of the AMO index together with tide gauge record of Forcado/ Nigeria
43
44 612 and the Ghana annual mean sea-level reconstruction
45
46
47
48
49
50
51

52 615 **LIST OF TABLES**

53

54
55 616 Table 1: Data used in this study with a summary description of their spatial resolution
56

57 617 Table 2: The percentage of the variance of the 4 leading EOFs of the annual mean SSH and
58
59 618 SST from the different sources used in this study data sets
60
61
62
63
64
65

Figure 1

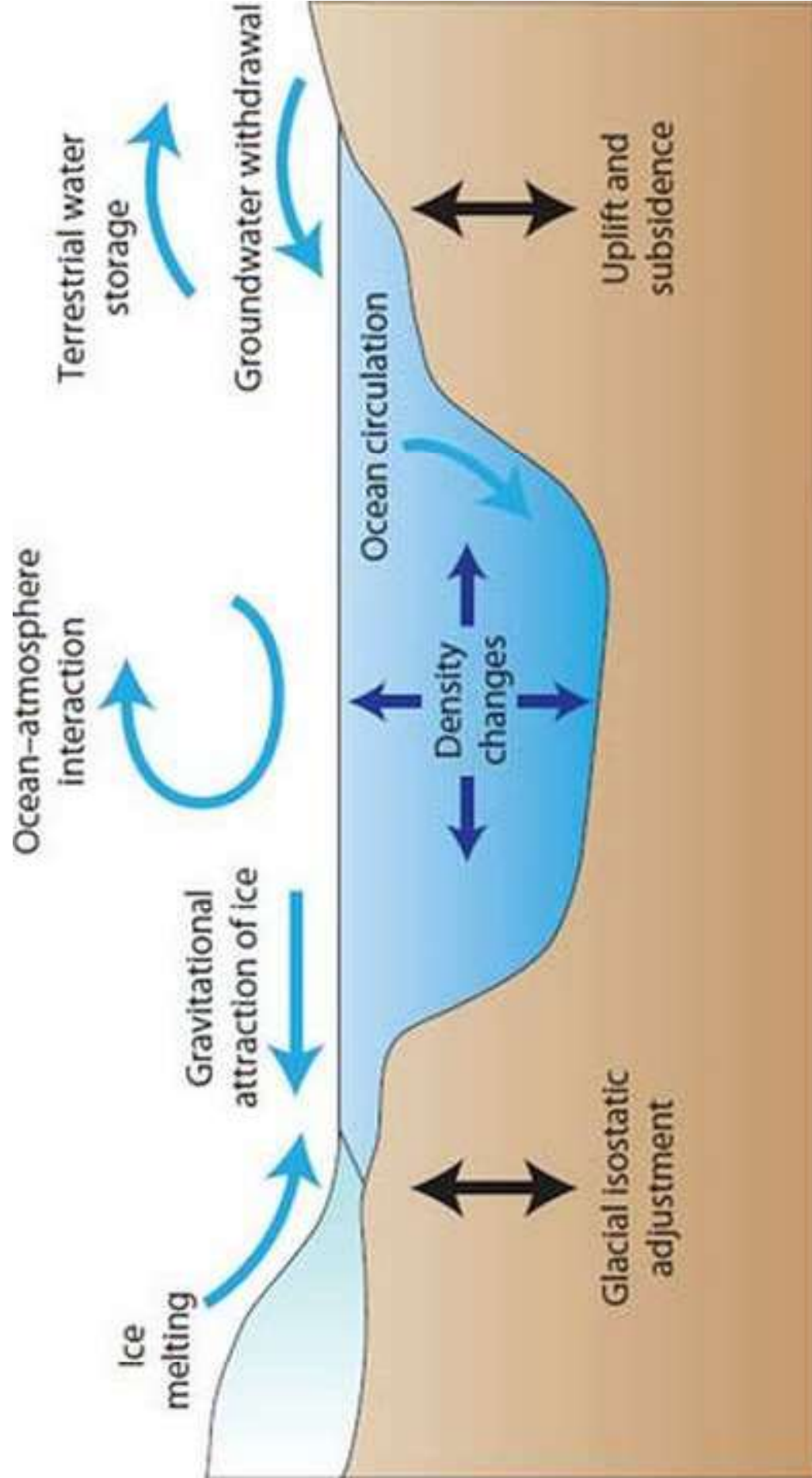


Figure 2

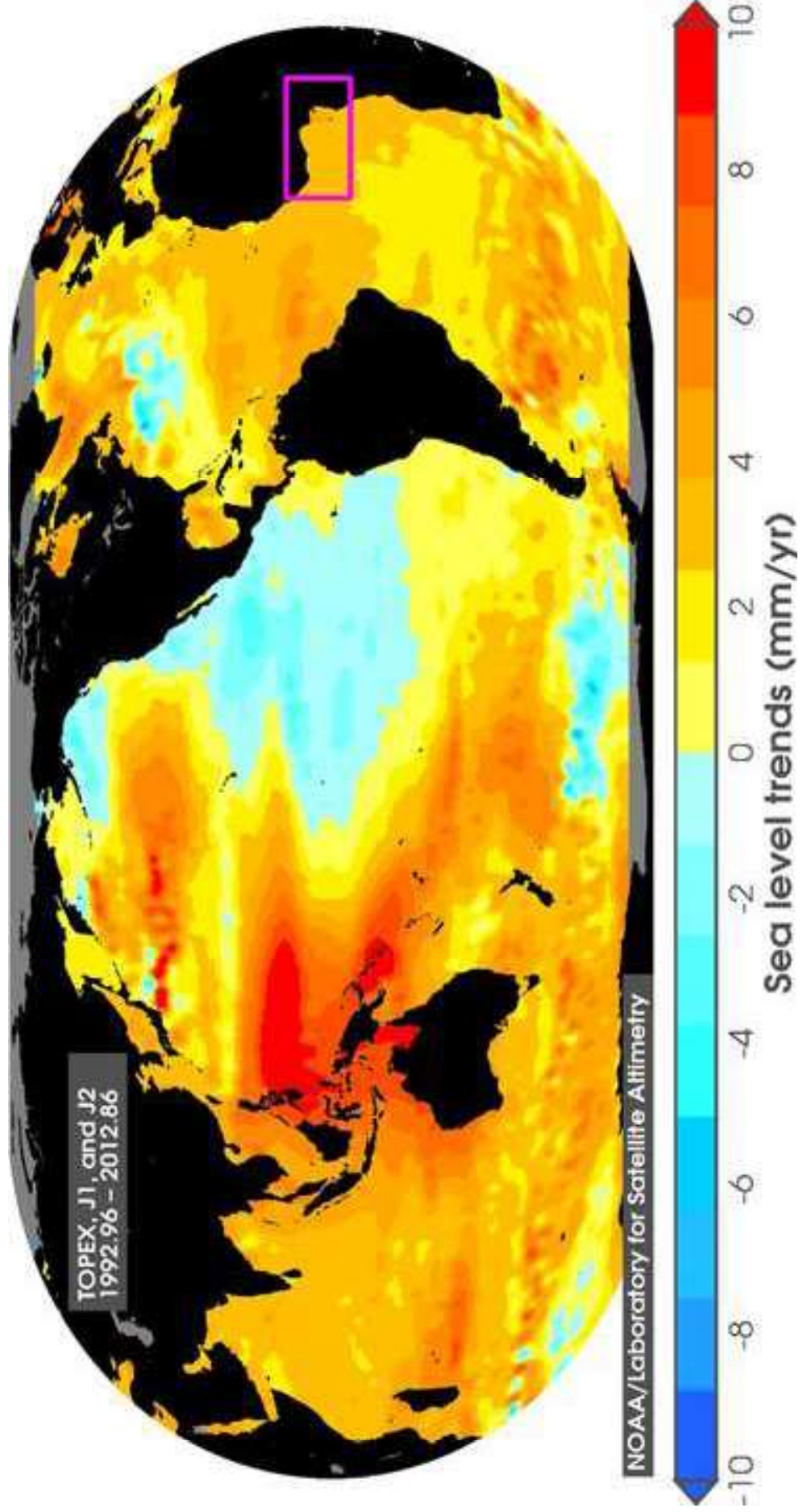
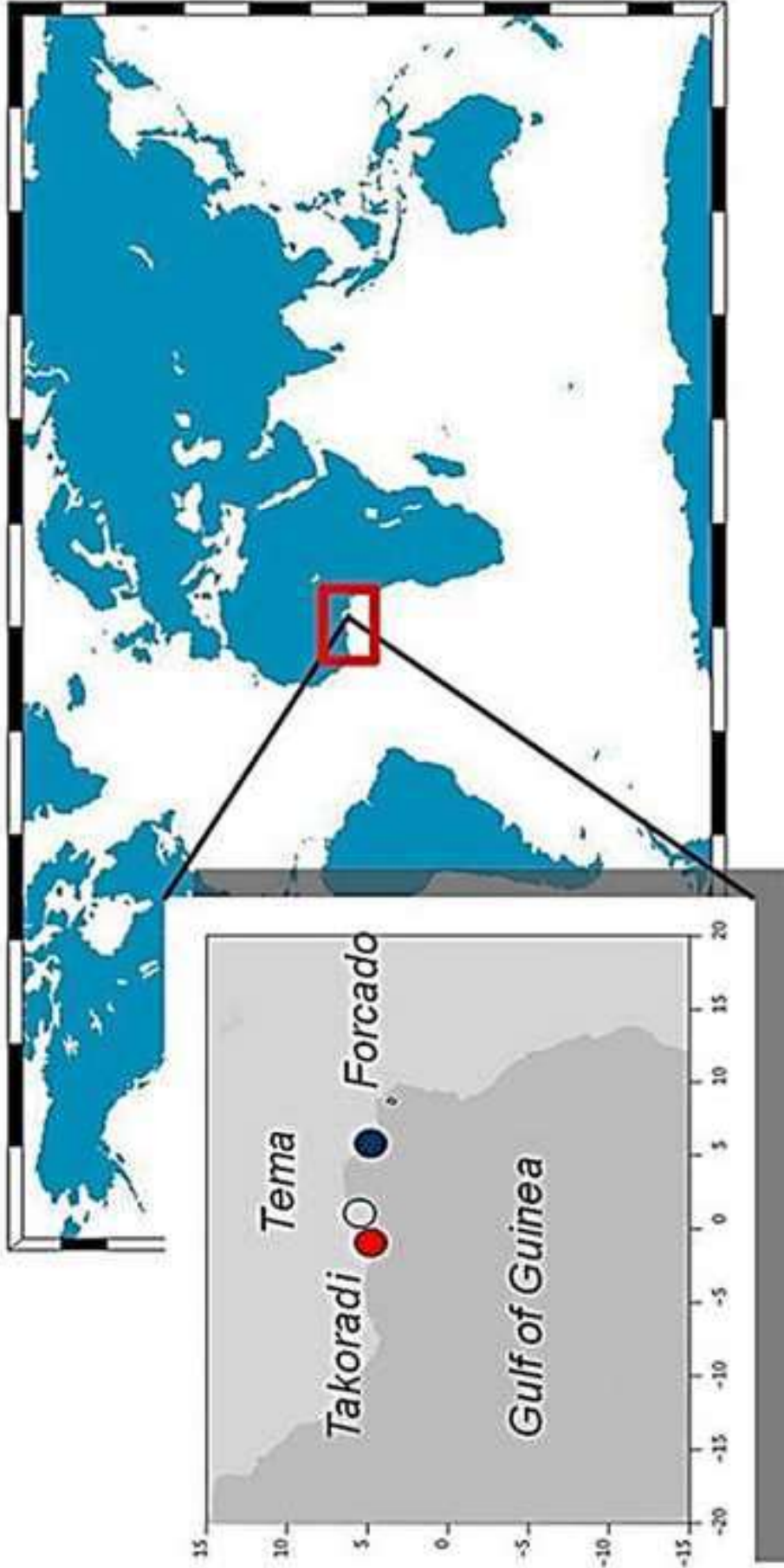


Figure 3



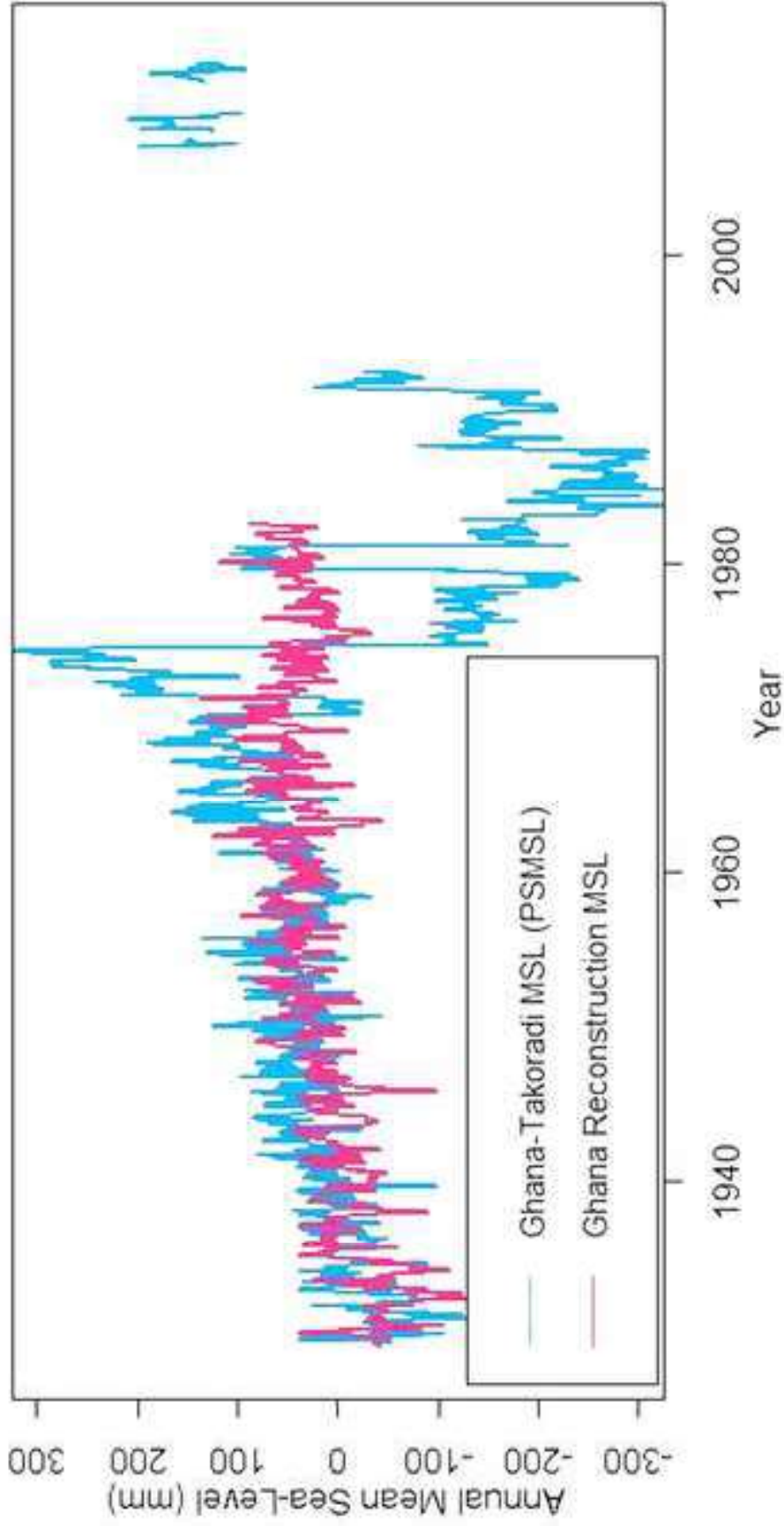


Figure 4

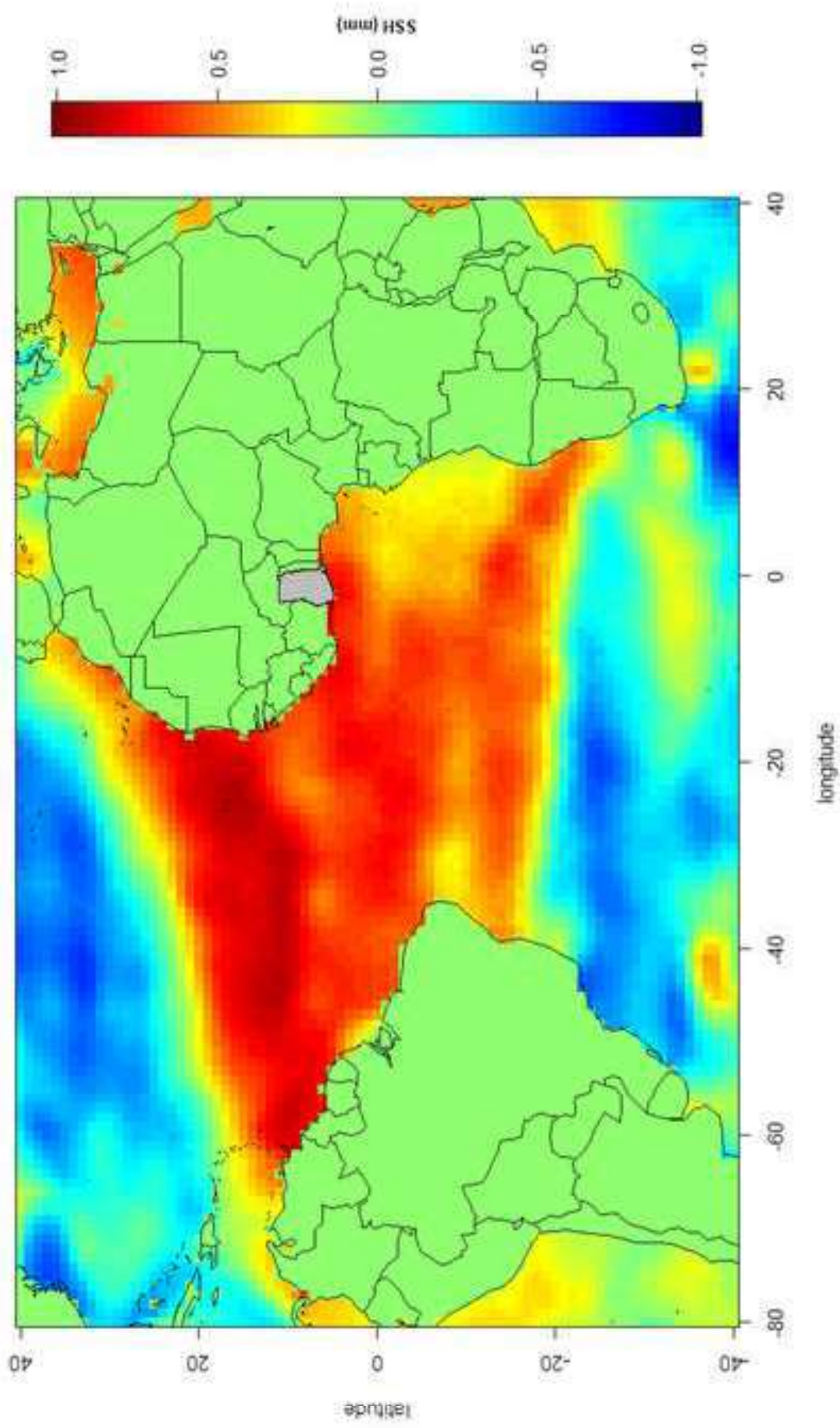


Figure 5a

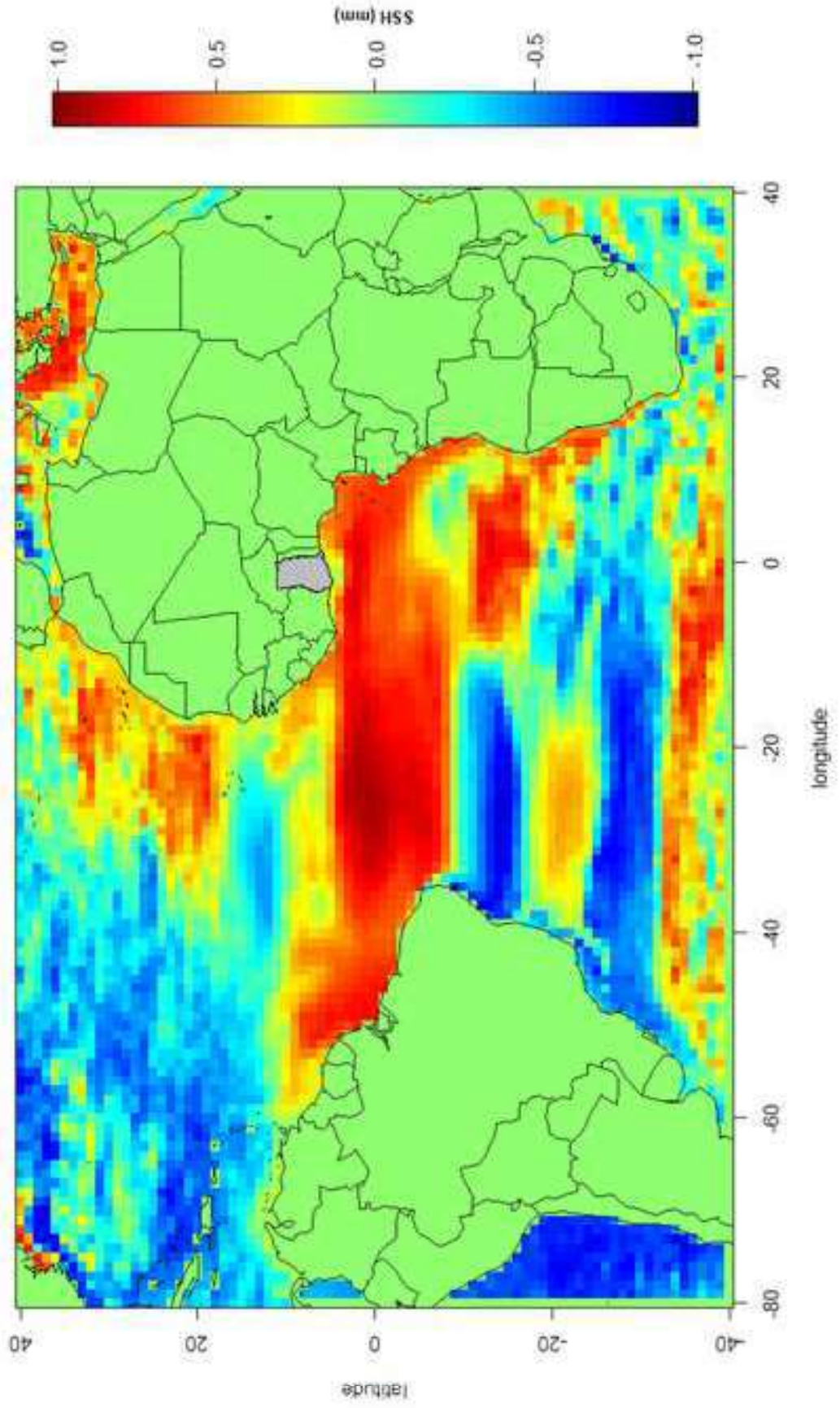


Figure 5b

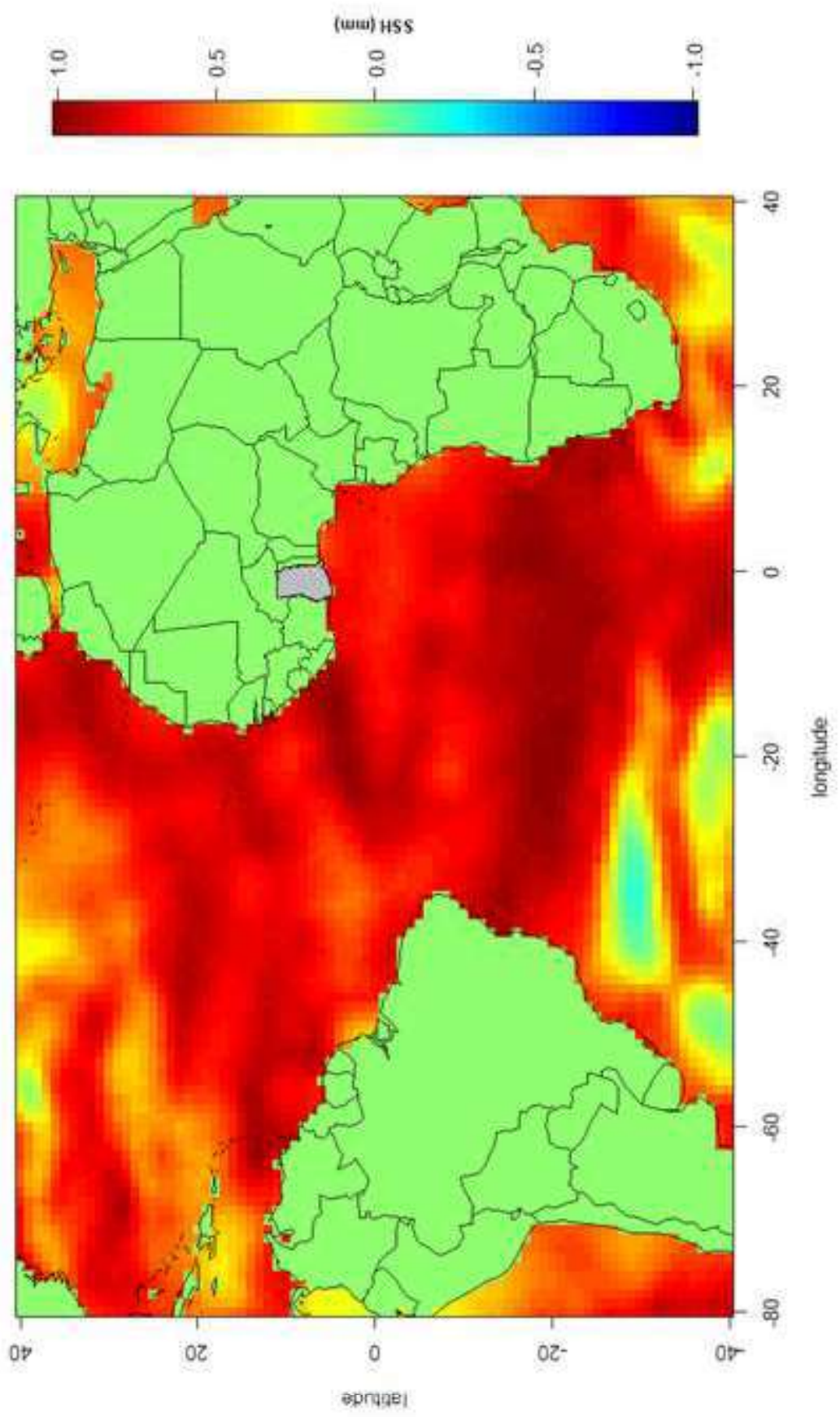


Figure 5c

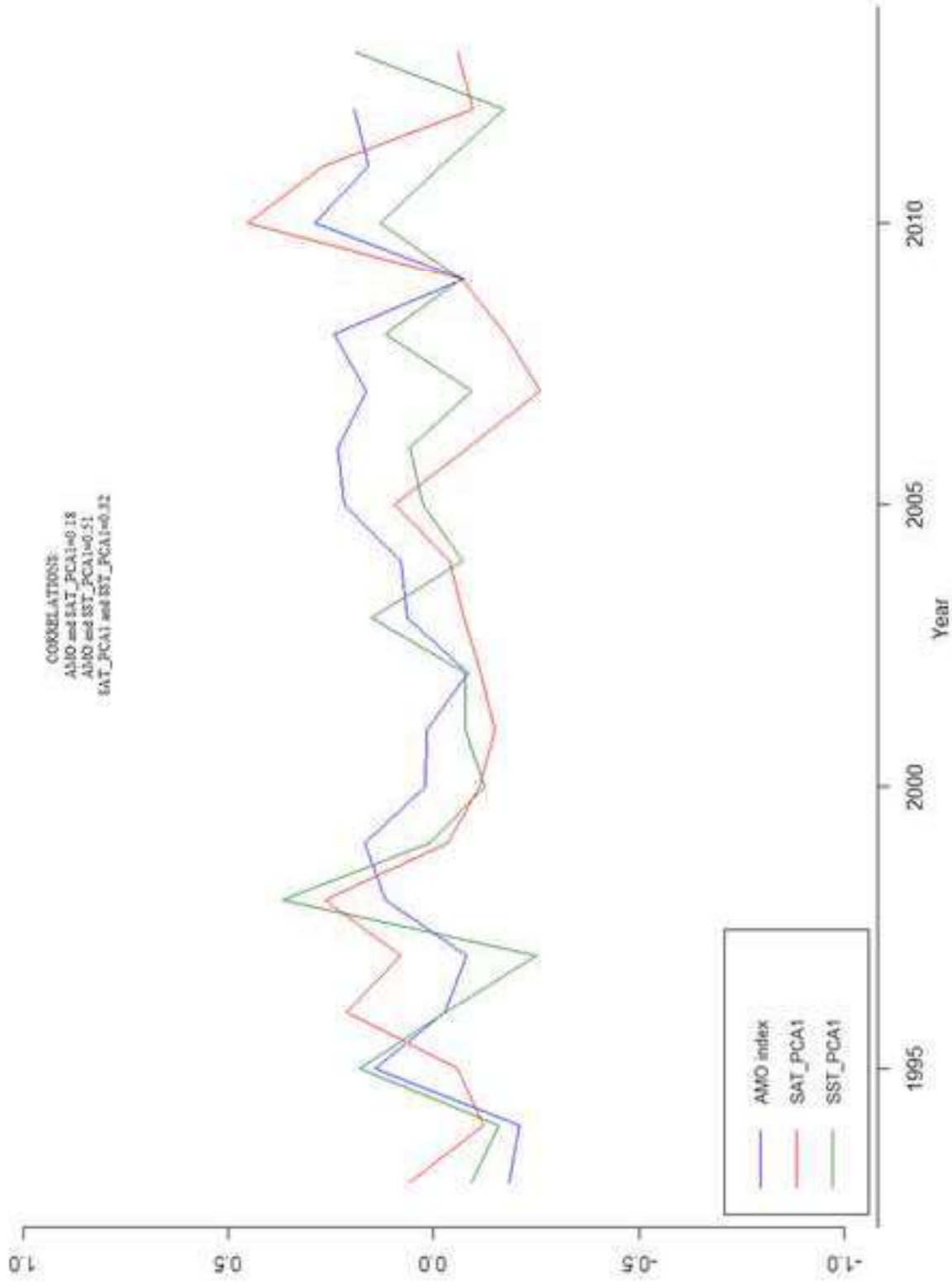


Figure 6

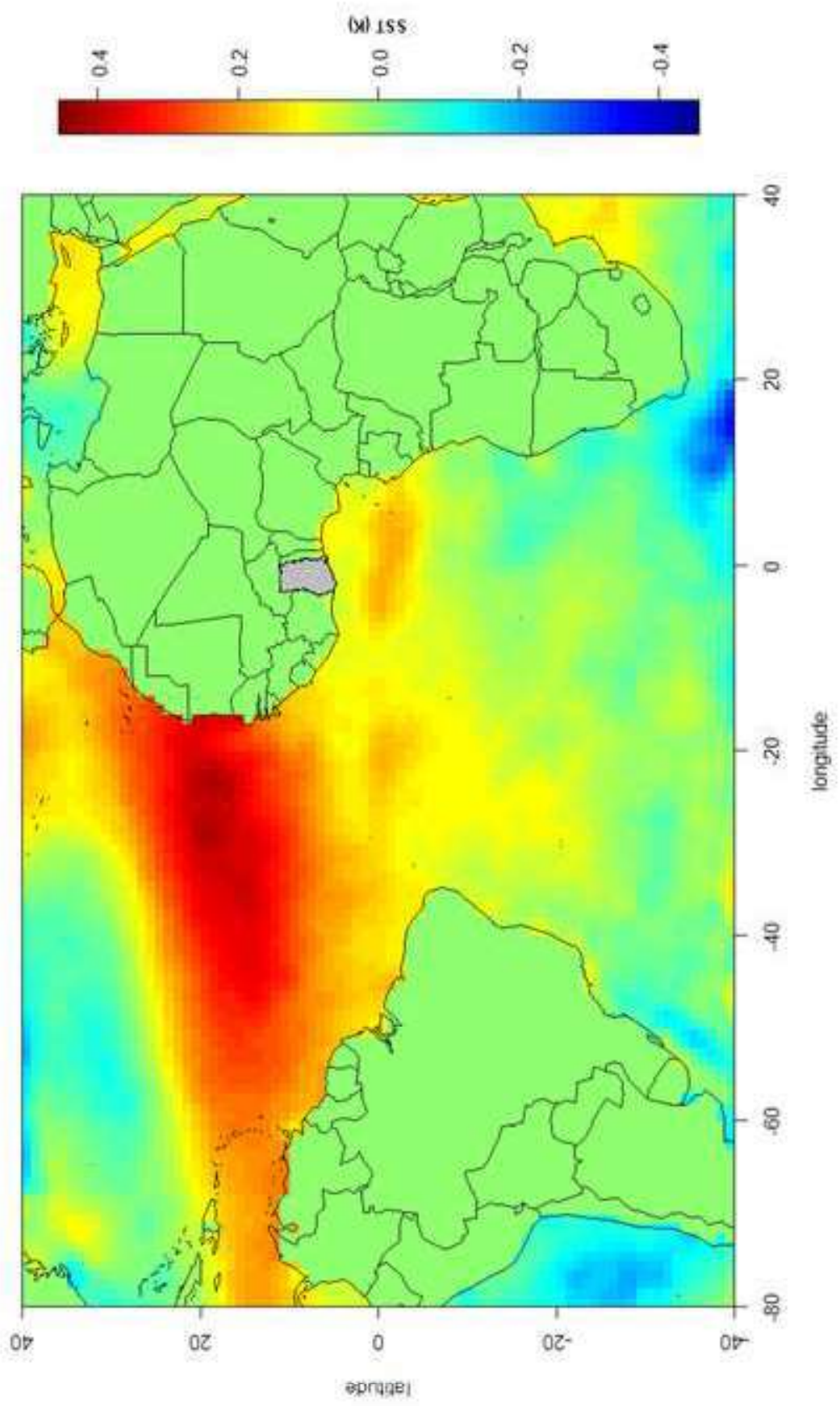


Figure 7a

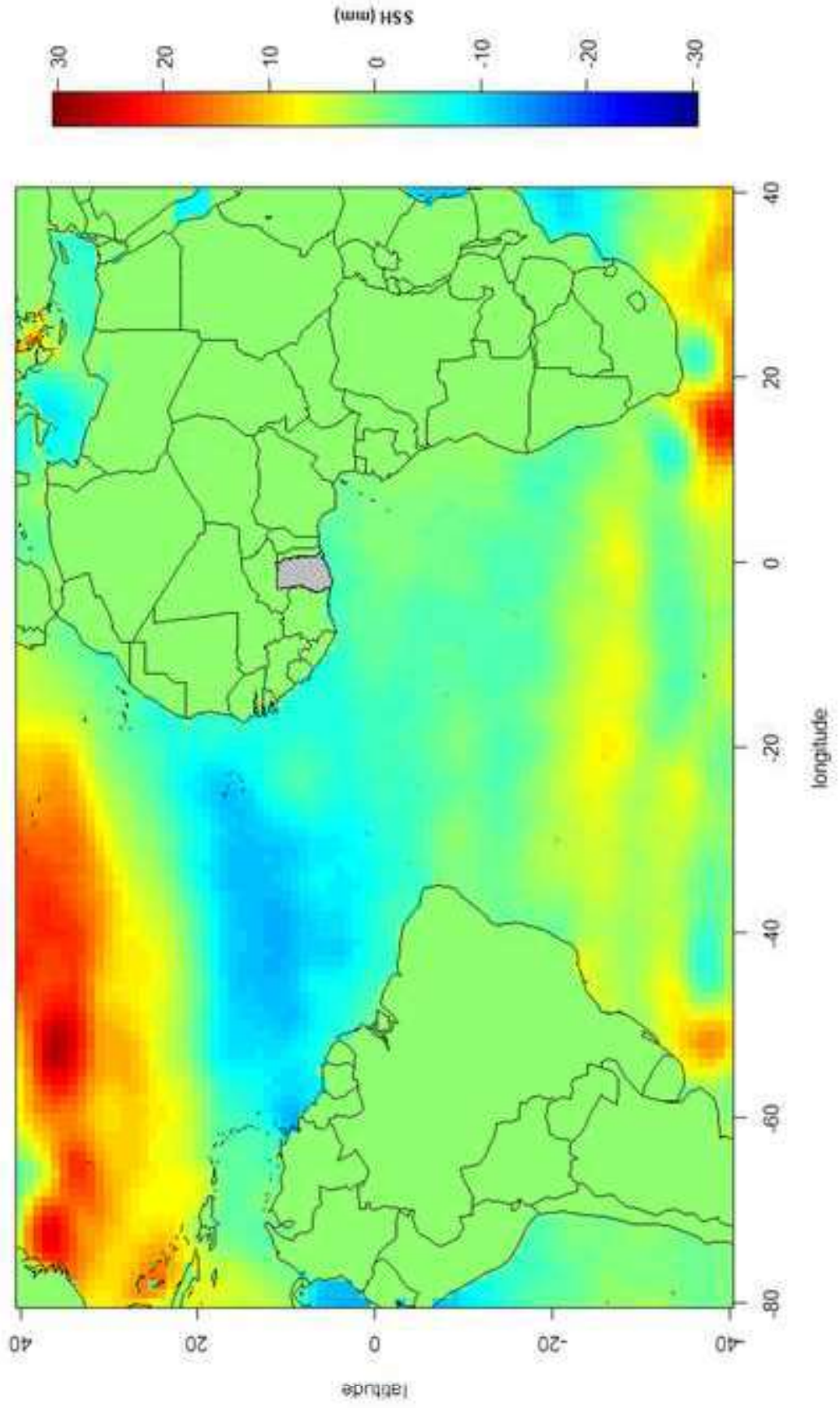


Figure 7b

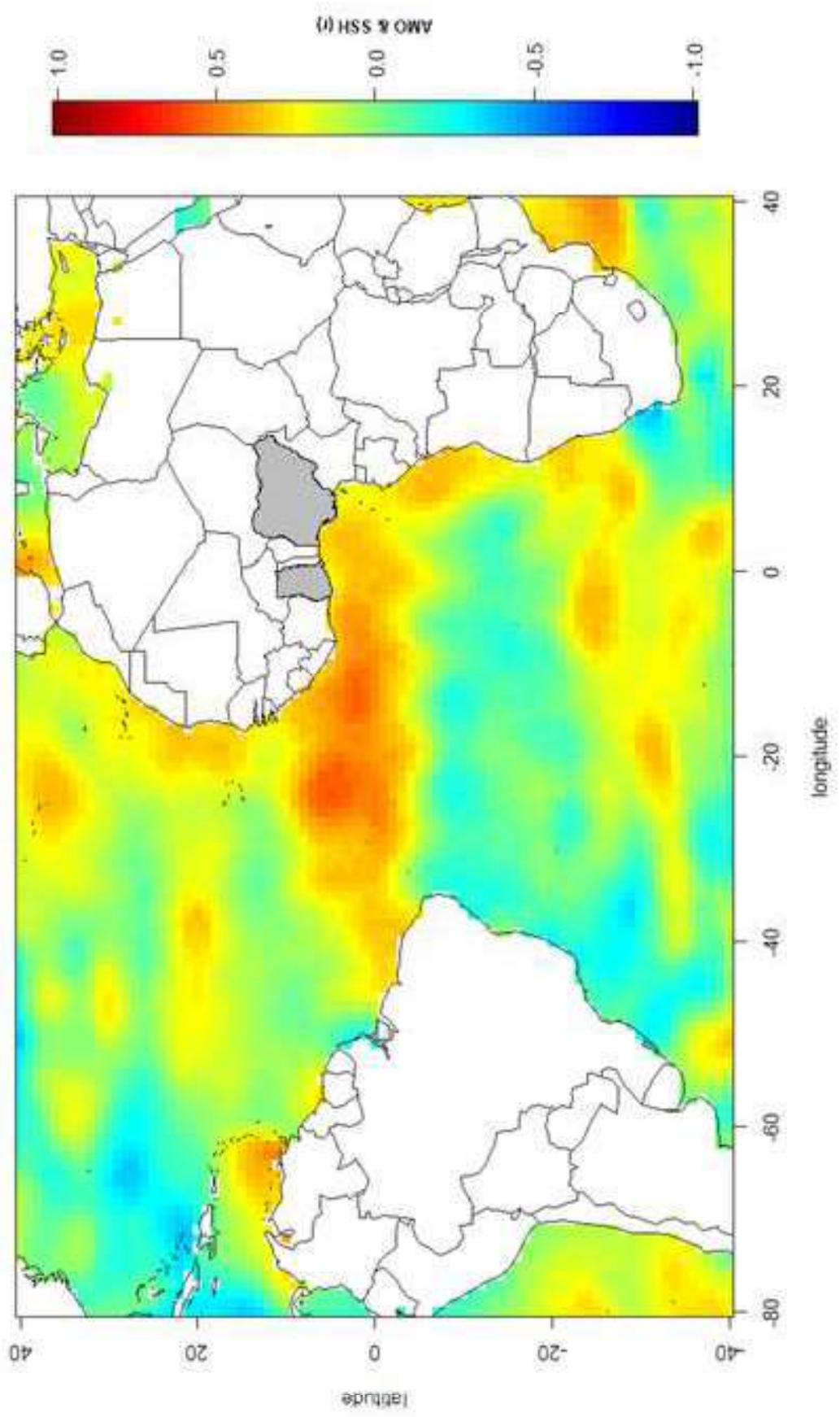


Figure 8

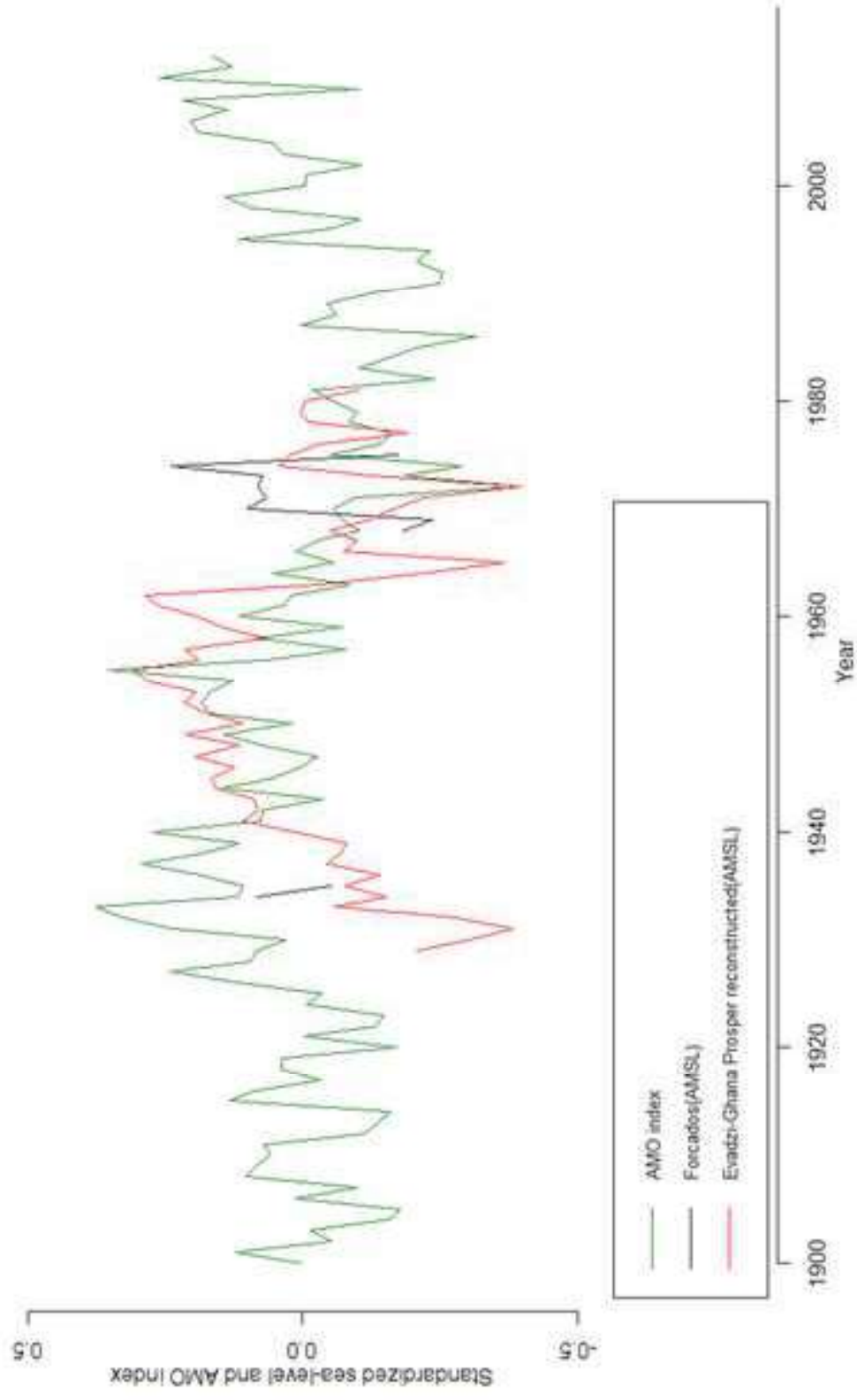


Figure 9

Table 1

Name/Acronym	Location/description	Years	Data source
SSH	near-global (65°S to 65°N), 1°×1° grid	1993-2013	Combined TOPEX/Poseidon, Jason-1 and Jason-2/OSTM sea-level fields
Monthly tide gauge data	Gulf of Guinea/ East Atlantic		PSMSL
Reconstructed SSH	near-global (65°S-65°N), 1°×1°×1month grid	1950-2001	Church et al. 2004
MPI-OM (STORM)	global ocean only simulation/model MPI-OM on a 0.1°×0.1° grid	1950-2010	Storch et al. 2012
HadISST 1	1° gridded global data	1870-2013	Rayner et al. 2003
AMO index	Index derived from HadSST (monthly mean)	1854-2012	http://climexp.knmi.nl/amo.cgi (Accessed 2014)
Wind stress	monthly gridded mean of momentum flux, U-component)	1948-2014	NCAR/NCEP Reanalysis. http://www.esrl.noaa.gov/psd/data/gridded/data.ncep.reanalysis.html (Accessed 2014)

Table 2

Data(scaled)	Components	% of variance
Satellite data(SSH)	Altimetry	
	EOF 1	20.22
	EOF 2	13.09
	EOF 3	10.86
MPI-OM (SSH)	EOF 4	9.29
	EOF 1	19.54
	EOF 2	13.28
	EOF 3	10.13
Church et al. (SSH)	EOF 4	7.72
	EOF 1	48.63
	EOF 2	15.04
	EOF 3	9.01
HadISST 1 (SST)	EOF 4	7.50
	EOF 1	21.37
	EOF 2	11.32
	EOF 3	9.91
	EOF 4	7.34